

# Chiral Electrodeposition

by Jay A. Switzer

Chirality is ubiquitous in Nature. One enantiomer of a molecule is often physiologically active, while the other enantiomer may be either inactive or toxic. For example, *S*-ibuprofen is up to 100 times more active than *R*-ibuprofen. *R*-thalidomide is a sedative, but *S*-thalidomide causes birth defects. Worldwide sales of single-enantiomer drugs reached \$159 billion in 2003.<sup>1</sup> The industrial synthesis of chiral compounds presently utilizes solution-phase, homogeneous catalysts and enzymes. Chiral surfaces offer the possibility of developing heterogeneous enantiospecific catalysts that can more readily be separated from the products and reused. In addition, such surfaces may serve as electrochemical sensors for chiral molecules, perhaps even implantable chiral sensors that could be used to monitor drug levels in the body. Another application would be post-chromatographic chiral electrochemical detectors, which would obviate the need for chiral separation of analyte molecules before chemical detection.

Chiral surfaces have been produced previously by adsorbing chiral molecules on achiral substrates,<sup>2-8</sup> or by slicing single crystals so that they exhibit high-index faces with chiral kink sites.<sup>9-17</sup> These high index single crystals have been shown to act as enantioselective heterogeneous catalysts.<sup>15</sup> Recently, we showed that chiral films of metal oxides such as CuO can be electrodeposited on achiral surfaces, using chiral molecules such as tartaric or amino acids to direct the chirality.<sup>18-20</sup> In this respect, electrodeposition resembles biomineralization in that organic molecules adsorbed on surfaces may have profound effects on the morphology of the inorganic deposits.<sup>17, 21-25</sup> The reduction of symmetry of surfaces by the adsorption of chiral molecules is known in biomineralization to produce chiral crystal habits on minerals such as calcite and gypsum which have achiral space groups. Enantioselective adsorption on the surfaces of minerals such as calcite has also been invoked to explain the genesis of biogenic homochirality.<sup>26</sup>

Our approach to the development of new chiral heterogeneous catalysts

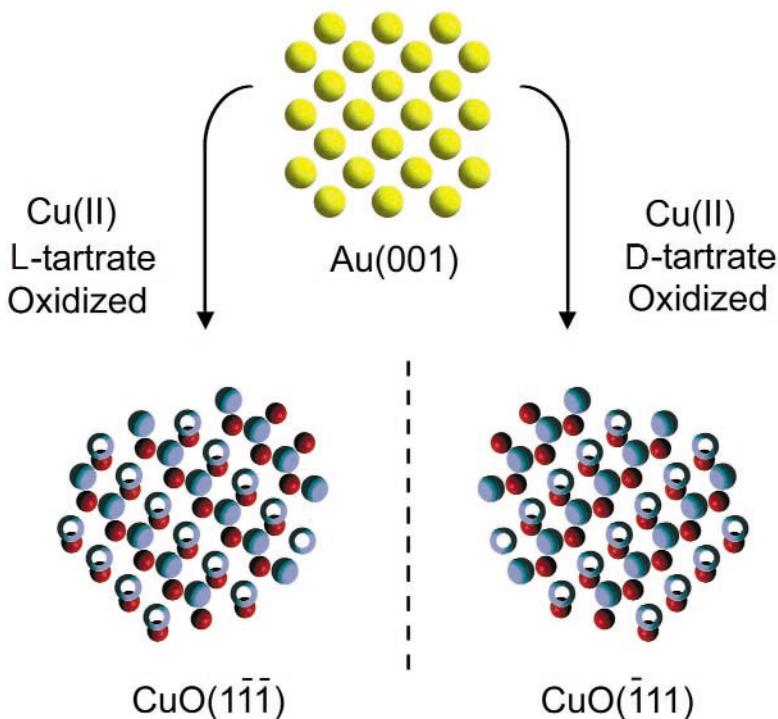


Fig. 1. Outline of the chiral electrodeposition scheme. Chiral CuO with either a  $(\bar{1}\bar{1}\bar{1})$  or  $(\bar{1}1\bar{1})$  orientation is electrodeposited onto achiral substrates such as Au(001). The  $(\bar{1}\bar{1}\bar{1})$  orientation is produced by oxidation of Cu(II) L-tartrate, and the  $(\bar{1}1\bar{1})$  orientation is produced by oxidation of Cu(II) D-tartrate. The two orientations of CuO lack mirror symmetry, and are clearly nonsuperimposable mirror images.

and sensors is to electrodeposit low symmetry metal oxide films with chiral orientations on achiral substrates. We have deposited chiral orientations of CuO on single-crystal Au and Cu using both tartaric acid and the amino acids alanine and valine to control the handedness of the electrodeposited films.<sup>18-20</sup> The use of chiral solution agents to control the chirality of electrodeposited films provides a degree of freedom that is not available to ultrahigh-vacuum vapor deposition methods. Previously, we showed that CuO can be electrodeposited by oxidizing Cu(II) complexes of tartaric acid,<sup>27</sup> and Nakaoka and Ogura have shown that the material can be produced by oxidizing Cu(II) complexes of amino acids.<sup>28</sup> An outline of the enantiospecific electrodeposition scheme for CuO on Au(001) is shown in Fig. 1. Chiral CuO with either a  $(\bar{1}\bar{1}\bar{1})$  or

$(\bar{1}1\bar{1})$  orientation is electrodeposited on Au(001). The films grown from L-tartaric acid [ $(R,R)$ -(+)-tartaric acid] have a CuO  $(\bar{1}\bar{1}\bar{1})$  orientation, while films grown from D-tartaric acid [ $(S,S)$ -(-)-tartaric acid] have a CuO  $(\bar{1}1\bar{1})$  orientation. The smaller dark red spheres at the bottom of Fig. 1 represent Cu atoms. There are two non-equivalent O atoms which are blue. The filled, blue O atoms are closest to the Cu plane, and sit in threefold hollow sites. The open, blue O atoms are nearly atop the Cu atoms. The two orientations of CuO are clearly nonsuperimposable mirror images. Polyhedral models of the two chiral orientations of CuO are shown in Fig. 2. In the image the  $(\bar{1}\bar{1}\bar{1})$  and  $(\bar{1}1\bar{1})$  planes are aligned parallel with the plane of the paper. The Cu atoms are shown in red, while the O atoms are shown in blue. The planes in light and dark blue

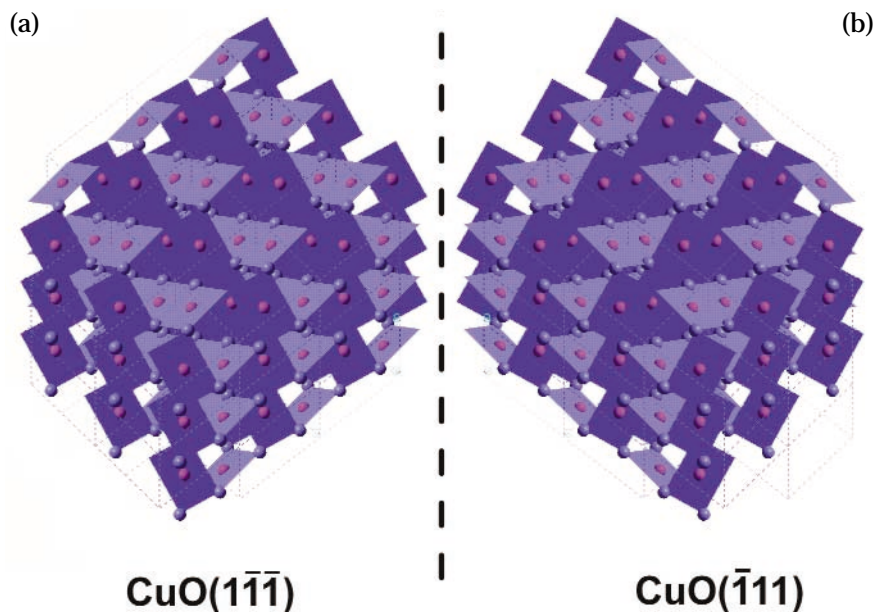


Fig. 2. Polyhedral models of the chiral  $(1\bar{1}\bar{1})$  and  $(\bar{1}11)$  orientations of CuO. The Cu atoms are shown in red, while the O atoms are shown in blue. The planes in light and dark blue show the Cu coordination with the nearest O atoms along the  $[110]$  and  $[\bar{1}10]$  directions.

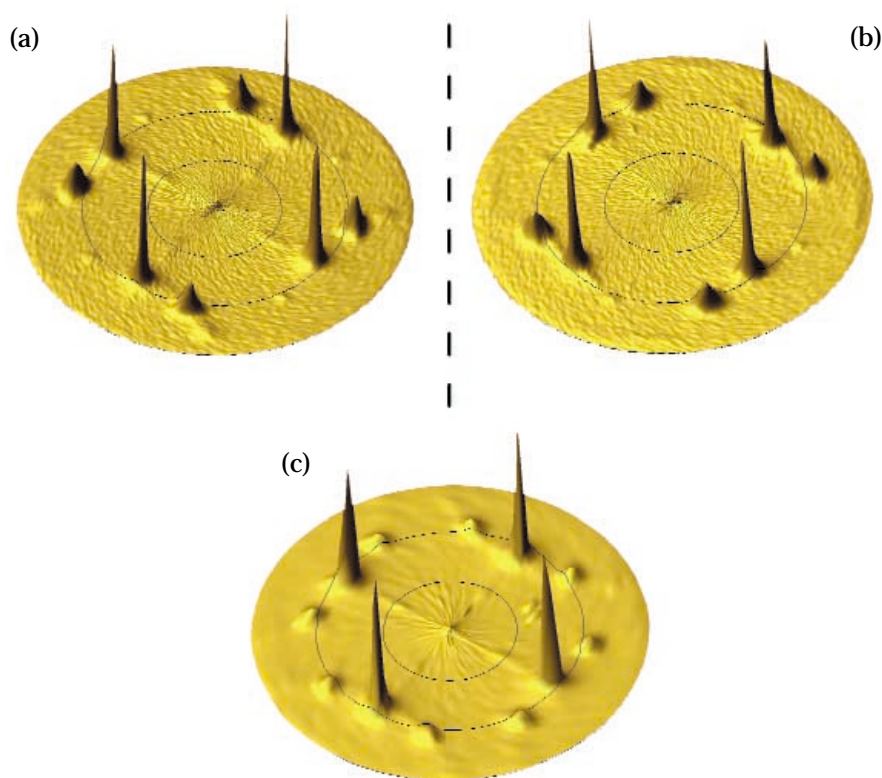


Fig. 3. CuO(111) X-ray pole figures for films of CuO on Au(001) grown from solutions of (a) L-tartaric acid, (b) D-tartaric acid, and (c) DL-tartaric acid. The film grown from L-tartaric acid has a  $(1\bar{1}\bar{1})$  orientation, while the film grown from D-tartaric acid has a  $(\bar{1}11)$  orientation. The film deposited from DL-tartaric acid has nearly equal amounts of the two chiral orientations.

show the Cu coordination with nearest O atoms along the  $[110]$  and  $[\bar{1}10]$  directions.

CuO can be deposited with chiral orientations even though the bulk crys-

tal structure of CuO is centrosymmetric. This is similar to the high-index faces of face-centered cubic (fcc) metals such as Cu and Pt. In these materials, the overall space group is centrosym-

metric, but orientations such as  $(643)$  and  $(\bar{6}\bar{4}\bar{3})$  are nonsuperimposable mirror images.<sup>9-17</sup> With lower symmetry materials such as CuO, it is not necessary to have large values for the Miller indices to observe chirality. Chiral crystal surfaces lack mirror or glide plane symmetry.<sup>29</sup> CuO has a monoclinic structure (space group  $C2/c$ ), with  $a = 0.4685$  nm,  $b = 0.3430$  nm,  $c = 0.5139$  nm, and  $\beta = 99.08^\circ$ . The unique twofold axis for CuO is the **b** axis, and the mirror plane is perpendicular to the **b** axis. Achiral orientations, therefore, correspond to those planes parallel with the **b** axis (planes of the  $[010]$  zone). Achiral planes are those with  $k = 0$ , such as  $(100)$ ,  $(101)$ ,  $(709)$ ,  $(001)$ , and, in the general case,  $(h0l)$ . Remaining planes with  $k \neq 0$ , such as  $(010)$ ,  $(111)$ , and  $(011)$  are all chiral. For an orientation which satisfies the conditions for chirality, the planes  $(hkl)$  and  $(\bar{h}\bar{k}\bar{l})$  form an enantiomorphic pair.

The absolute configuration of chiral films can be determined by X-ray pole figure analysis. Pole figures can be used to probe planes that are not parallel with the geometric plane of the sample. The sample is moved through a series of tilt angles,  $\chi$ , and at each tilt angle the sample is rotated through azimuthal angles,  $\varphi$ , of 0 to  $360^\circ$ . Peaks occur in the pole figure when the Bragg condition is satisfied. The pole figure determines both the out-of-plane and in-plane orientations of the film, in addition to the orientation of the film relative to the substrate. Figure 3 shows  $(111)$  pole figures for 300 nm thick CuO films deposited on a Au(001) single crystal from solutions of (a) L-tartaric acid, (b) D-tartaric acid, and (c) DL-tartaric acid. The radial direction is the tilt of the sample with grid lines spaced  $30^\circ$  apart. The films grown from L-tartaric acid have a CuO $(1\bar{1}\bar{1})$  orientation, while films grown from D-tartaric acid have a CuO $(\bar{1}11)$  orientation. With the intense Au peaks at  $\chi = 54.7^\circ$  acting as an internal reference, it is evident that Fig. 3a and b are nonsuperimposable mirror images of each other. Therefore, the two orientations are enantiomorphs. Figure 3c shows that a CuO film grown from a racemic mixture of tartaric acid has equal amounts of the two enantiomeric orientations.

The enantiomeric excess of one orientation over the other may also be determined by X-ray diffraction (XRD)

using azimuthal scans. Figure 4 shows azimuthal scans extracted from the (111) pole figures in Fig. 3 at  $\chi = 63^\circ$  with the azimuthal angle,  $\phi$ , varying from 60 to 120°. The peaks in blue and red correspond to the  $(\bar{1}\bar{1}\bar{1})$  and  $(\bar{1}\bar{1}1)$  orientations, respectively. The film produced from L-tartaric acid has the  $(\bar{1}\bar{1}\bar{1})$  orientation in 95% enantiomeric excess, while the film produced from D-tartaric acid has the  $(\bar{1}\bar{1}1)$  orientation in 93% enantiomeric excess. The film deposited from DL-tartaric acid has equal amounts of both orientations and has essentially zero enantiomeric excess.

Other chiral agents besides tartaric acid can be used as templates for chiral electrodeposition. We have used amino acids such as valine and alanine to deposit chiral CuO films on single-crystal Au and Cu. Figure 5 shows (111) pole figures for CuO deposited on Cu(110) from D-alanine and L-alanine. CuO films deposited from D-alanine (Fig. 5a) grow with the  $(\bar{1}\bar{1}\bar{0})$  orientation, while films deposited from L-alanine (Fig. 5b) grow with the (110) orientation. These orientations both lack mirror symmetry and are nonsuperimposable mirror images of each other. CuO films grown from either DL-alanine or the achiral amino acid glycine consist of a racemic mixture of the  $(\bar{1}\bar{1}\bar{0})$  and (110) orientations.

The X-ray pole figures show that the bulk films grown in tartaric or amino acids are enantiomers, but they do not provide information on the chirality of the surface. Electrochemical oxidation studies were done to probe the surface chirality. CuO has been shown by other workers to be a potent electrocatalyst for the oxidation of carbonates, amino acids, simple alcohols, aliphatic diols, and alkyl polyethoxy alcohol detergents.<sup>30</sup> Cyclic voltammograms (CVs) showing the oxidation of tartaric acid on CuO deposited from L-, D-, and DL-tartaric acid onto Au(001) are shown in Fig. 6. The chiral recognition studies were run in a solution containing 5 mM tartaric acid in 0.1 M NaOH. The CVs were obtained in unstirred solutions by scanning from the rest potential to +0.75 V vs. a saturated calomel electrode (SCE) at a scan rate of 10 mV/s. Before switching solutions the electrode was cleaned by scanning in 0.1 M NaOH. Oxidation of the solvent occurs at about 0.6 V vs. SCE on the CuO electrodes (dotted curves in Fig. 6). The CVs show that films grown in L-tartaric acid (Fig. 6a) selectively oxidize L-tartaric acid, while films grown in D-tartaric acid (Fig. 6b) selectively oxidize D-tar-

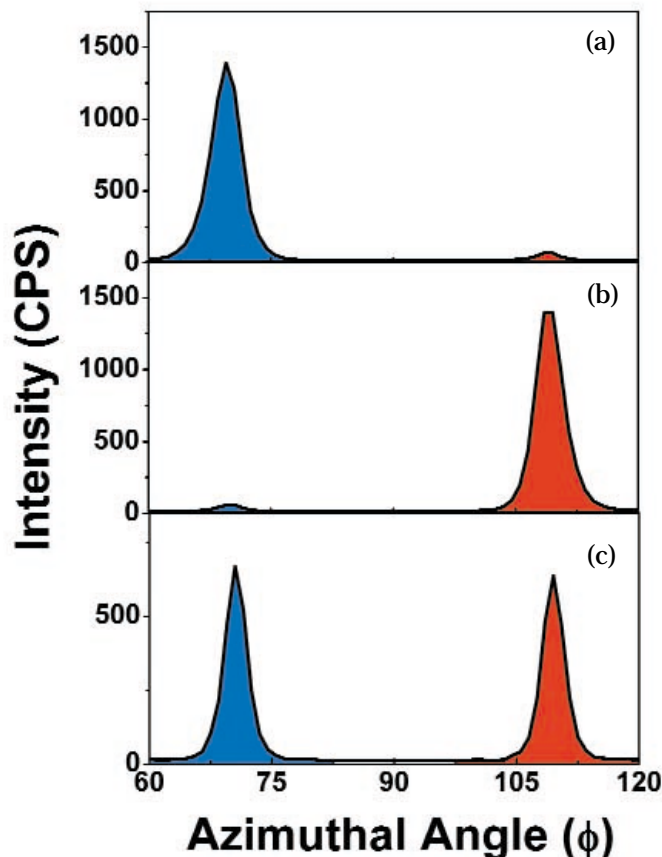


Fig. 4. Determination of the enantiomeric excess (*ee*) of the CuO chiral orientations on Au(001) using X-ray diffraction azimuthal scans. The azimuthal scans probe the {111} reflections of CuO at a tilt angle of 63° for CuO films grown from (a) L-tartaric acid, (b) D-tartaric acid, and (c) DL-tartaric acid. The film produced from L-tartaric acid has the  $(\bar{1}\bar{1}\bar{1})$  orientation in 95% *ee*, while the film produced from D-tartaric acid has the  $(\bar{1}\bar{1}1)$  orientation in 93% *ee*. CuO deposited from DL-tartaric acid has equal amounts of both orientations, and has essentially zero *ee*.

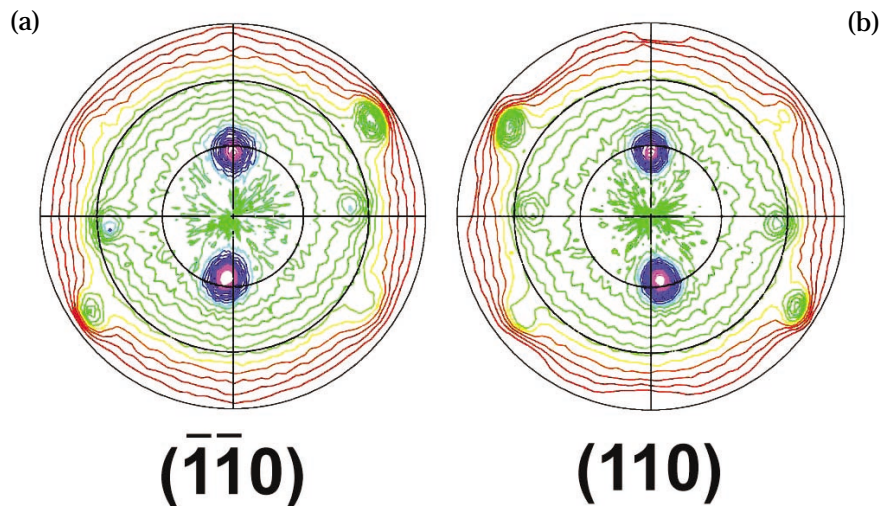


Fig. 5. CuO(111) pole figures for films of CuO on Cu(110) grown from solutions of (a) D-alanine and (b) L-alanine. The film grown from D-alanine has a  $(\bar{1}\bar{1}\bar{0})$  orientation, while the film grown from L-alanine has a (110) orientation. The two orientations are nonsuperimposable mirror images. Films of CuO deposited from either DL-alanine or the achiral amino acid glycine are achiral.

taric acid. A film grown in DL-tartaric acid (Fig. 6c) shows no selectivity. Chiral recognition of tartaric acid is also observed for films deposited from amino

acids. In this case, films deposited from D-amino acids are selective for the oxidation of L-tartaric acid, and films deposited from L-amino acids are selec-

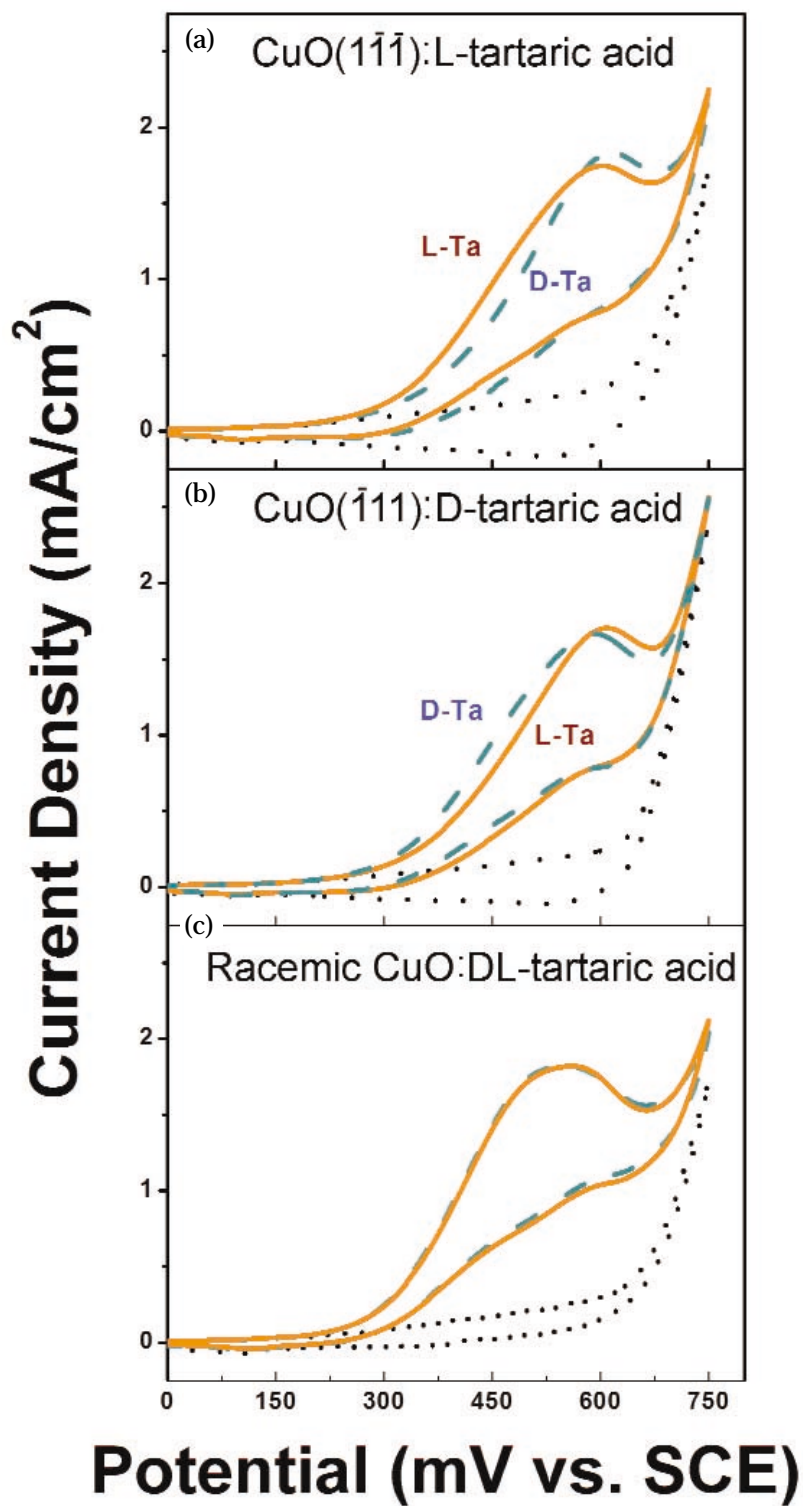


FIG. 6. Chiral recognition of tartaric acid by chiral CuO deposited on Au(001). CVs were run at room temperature in solutions of 5 mM L-tartaric acid (solid orange line) or 5 mM D-tartaric acid (dashed cyan line) in 0.1 M NaOH for CuO films deposited in (a) L-tartaric acid, (b) D-tartaric acid, and (c) DL-tartaric acid. The film grown from L-tartaric acid selectively oxidizes L-tartaric acid over D-tartaric acid, while the film grown from D-tartaric acid selectively oxidizes D-tartaric acid over L-tartaric acid. The control experiment in part (c) on an achiral CuO film shows no enantioselectivity.

tive for the oxidation of D-tartaric acid. Chiral recognition studies of other molecules on the chiral CuO surfaces are currently underway in our group.

We have shown that chiral films of CuO can be deposited on achiral Au and Cu substrates. Typical of research, there are now more unanswered questions

than solutions. How general is chiral electrodeposition? Because the only requirement for materials to be chiral is that the surface does not contain mirror or glide planes, there is a huge number of materials that may be used to produce chiral surfaces. How does chiral electrodeposition work? Much more research must be done to understand the mechanism of chiral electrodeposition. Obviously, the chiral solution agents are directing the growth, but the templating or imprinting mechanisms are unclear. Also, what molecules beside tartaric acid can be differentiated on these surfaces? Will these surfaces be used to produce practical chiral catalysts, sensors, or detectors? We invite the scientific community to help answer these questions.

### Acknowledgments

This work was supported by NSF grants CHE-0243424, CHE-0437346, DMR-0071365, and DMR-0076338, U.S. Department of Energy grant DE-FC07-03ID14509, and the Foundation for Chemical Research. The author also acknowledges the graduate students and postdoctoral associates who did the work reported here. These researchers are (listed alphabetically) Eric W. Bohannon, Sansanee Boonsalee, Hiten M. Kothari, Elizabeth A. Kulp, Run Liu, Shuji Nakanishi, Igor M. Nacic, Maxim P. Nikiforov, and Philippe Poizot. ■

### References

1. A. M. Rouhi, *Chem. Eng. News*, **82**, 47 (2004).
2. M. O. Lorenzo, C. J. Baddeley, C. Muryn, and R. Raval, *Nature*, **404**, 376 (2000).
3. V. Humblot, S. Haq, C. Muryn, W. A. Hofer, and R. Raval, *J. Am. Chem. Soc.*, **124**, 503 (2002).
4. S. M. Barlow, S. Louafi, D. Le Roux, J. Williams, C. Muryn, S. Haq, and R. Raval, *Langmuir*, **20**, 7171 (2004).
5. R. B. Rankin and D. S. Sholl, *Surf. Sci.*, **548**, 301 (2004).
6. A. Kühnle, T. R. Linderoth, B. Hammer, and F. Besenbacher, *Nature*, **415**, 891 (2002).
7. Y. Izumi, in *Advances in Catalysis*, Vol. 32, p. 215, Academic, New York (1983).
8. C. LeBlond, J. Wang, J. Liu, A. T. Andrews, and Y.-K. Sun, *J. Am. Chem. Soc.*, **121**, 4920 (1999).
9. C. F. McFadden, P. S. Cremer, and A. J. Gellman, *Langmuir*, **12**, 2483 (1996).
10. J. D. Horvath and A. J. Gellman, *J. Am. Chem. Soc.*, **123**, 7953 (2001).
11. J. D. Horvath and A. J. Gellman, *J. Am. Chem. Soc.*, **124**, 2384 (2002).
12. A. Ahmadi, G. Attard, J. Feliu, and A. Rodes, *Langmuir*, **15**, 2420 (1999).
13. G. A. Attard, A. Ahmadi, J. Feliu, A. Rodes, E. Herrero, S. Blais, and G. Jerkiewicz, *J. Phys. Chem. B*, **103**, 1381 (1999).
14. G. A. Attard, *J. Phys. Chem. B*, **105**, 3158 (2001).
15. O. A. Hazzazi, G. A. Attard, and P. B. Wells, *J. Mol. Catal. A: Chem.*, **216**, 247 (2004).
16. D. S. Sholl, A. Asthagiri, and T. D. Power, *J. Phys. Chem. B*, **105**, 4771 (2001).

(continued on next page)

